INTERNATIONAL JOURNAL FOR NUMERICAL METHODS IN FLUIDS, VOL. 3, 429–443 (1983)

A TRANSIENT FINITE ELEMENT ANALYSIS OF NATURAL CONVECTION AROUND A HORIZONTAL HOT CYLINDER

YASUYUKI MIYAUCHI,* MICHIO MASUDA AND MASATSUGU SHIMIZU

Tokai Research Establishment, Division of Large Tokamak Development, Japan Atomic Energy Research Institute, Tokai-mura, Ibaraki 319-11, Japan

SUMMARY

This paper presents an advanced method for a 2-dimensional analysis of transient natural convection by finite element method. The present method, based on stream function–vorticity formulation, could get rid of numerical errors and constraint of perpendicular mesh subdivision, since we excluded a finite difference approximation of vorticity on no-slip boundaries. A considerable effect of upwind weighting function was examined. The method was successfully applied to a problem of natural convection around a horizontal hot cylinder.

KEY WORDS Natural Convection Finite Element Method Upwind Finite Element Cylinder

1. INTRODUCTION

The thermal design of the large tokamak JT-60, which is under construction at JAERI, showed some difficulties related to natural convection. When the vacuum vessel is heated up, the air flow induced at the surface of the thermal insulator covering the vessel may bring troubles with diagnostics and with the electric insulator of the poloidal magnetic field coils, located over and around the vessel. Therefore, it is necessary to analyse, in detail, the natural convection of air around the vacuum vessel, in order to determine the maximum allowable baking and operation temperature and to design heat removing equipments. For this purpose, we developed a 2-dimensional finite element code which analyses transient natural convection.

There are two major computational methods for fluid simulation: finite difference method (FDM) and finite element method (FEM). Application of FDM to fluid dynamics has been studied and established from the early days of computer simulation and many interesting results[1–3] including those of natural convection have been published. Davis and Mallinson[4] numerically showed the secondary and tertiary flow of natural convection in a rectangular cavity which had been experimentally observed by Elder.[5] Mallinson and Davis[6] performed 3-dimensional computation using what they called the false transient method. Pepper and Harris[7] and Torrance and Rockett[8] reported their calculations of axi-symmetric time dependent problems. However, FDM requires complicated techniques[3] for geometrically complicated problems. Indeed, it will be practically impossible to analyse the natural convection for a complicated geometry like that around the JT-60 vacuum vessel by FDM.

* Ishikawajima-Harima Heavy Industries Co., Ltd., Ote-machi, Chiyoda-ku, Tokyo 100, Japan

0271–2091/83/050429–15$01.50

Received 1 October 1981
Revised 23 July 1982

On the other hand, FEM, whose application to fluid dynamics has been intensively studied only in the last ten years,[9–13] has the advantage that it can analyse arbitarily shaped regions in a uniform manner. As most of the numerical studies of natural convection make the Boussinesq approximation which treats the fluid as incompressible, the formulation based on stream function and vorticity has conventionally been used for such studies.[13] But, such a formulation has the disadvantage, for practical application, that the mesh subdivision on no-slip boundaries is restricted to be perpendicular for finite difference approximation of vorticity on such boundaries.[9–11] The restriction obviously reduces practical convenience and induces some numerical errors.

We exclude this restriction by the use of the equation of motion for the stream function instead of the vorticity. This method has been successfully applied by Ikenouchi and Kimura[14] to the Navier–Stokes equation without body force. We extend the method to the basic equations of transient natural convection. The equations are discretized by the Galerkin method. The advantage of an upwind weighting function[9] is also checked. We use explicit time integration methods: the Euler method and the 2-step Lax–Wendroff method. In order to justify the present method, we compare our numerical result for natural convection induced by a hot wall of a closed cavity with the result of Reddy and Satake.[13] We also demonstrate a time dependent evolution of the convective flow induced by a horizontal hot cylinder, as the preparation of numerical analysis of the air convection around JT-60.

2. FINITE ELEMENT FORMULATION

2.1. Basic equations

It is common to use the Boussinesq approximation for the study of natural convection. The approximation treats small deviations of pressure and temperature from their ambient values, and the fluid itself is considered to be incompressible. The thermal transport equation must be directly coupled with the momentum transport equation, because the buoyancy force, caused by the temperature distribution, is the dominant motive force of this system. The basic equations of natural convection can be written as follows.

Momentum transport equation:

$$\frac{\partial \mathbf{v}}{\partial t}+(\mathbf{v}\cdot\nabla)\mathbf{v}+\frac{1}{\rho}\nabla p-\nu\nabla^2\mathbf{v}+\beta\mathbf{g}T=0 \tag{1}$$

Equation of incompressibility:

$$\nabla\cdot\mathbf{v}=0 \tag{2}$$

Thermal transport equation:

$$\frac{\partial T}{\partial t}+(\mathbf{v}\cdot\nabla)T-a\nabla^2T=0 \tag{3}$$

Although the incompressibility is formally represented by equation (2), density may vary as a material property according to the temperature. This way of treating density is indispensable for the analysis of problems of gas flows with wide temperature distribution.

Equation (2) indicates that the velocity can be represented by a vector potential as

$$\mathbf{v}=\nabla\times\boldsymbol{\Psi} \tag{4}$$

As only two of the three components of velocity are independent in a 2-dimensional analysis, we set the following condition on $\boldsymbol{\Psi}$ in order to reduce the number of its degrees of freedom.

$$\nabla \cdot \boldsymbol{\Psi} = 0 \tag{5}$$

The vorticity vector, defined by

$$\boldsymbol{\omega} = \nabla \times \mathbf{v} \tag{6}$$

can be represented in terms of $\boldsymbol{\Psi}$ as

$$\boldsymbol{\omega} = -\nabla^2 \boldsymbol{\Psi} \tag{7}$$

Then the curl of equation (1) gives

$$-\frac{\partial}{\partial t}(\nabla^2 \boldsymbol{\Psi}) + (\mathbf{v} \cdot \nabla)\boldsymbol{\omega} - (\boldsymbol{\omega} \cdot \nabla)\mathbf{v} - \nu \nabla^2 \boldsymbol{\omega} + \beta \nabla T \times \mathbf{g} = 0 \tag{8}$$

Hence, the set of independent variables $\mathbf{v}$, p, and T can be replaced by the set of $\boldsymbol{\Psi}$ and T, and this considerably economizes computing effort, computer memory and time.

2.2. *Non-dimensional formulation*

We non-dimensionalize the variables and symbols as

$$\begin{aligned} &\nabla = L^{-1}\nabla^*, \qquad \mathbf{v} = U\mathbf{v}^*, \qquad \frac{\partial}{\partial t} = L^{-1}U\frac{\partial}{\partial t^*}, \qquad \mathbf{g} = g\mathbf{g}^* \\ &p = \rho U^2 p^*, \qquad T = (\Delta T)\theta + T_\infty, \qquad \boldsymbol{\Psi} = LU\boldsymbol{\Psi}^*, \qquad \omega = L^{-1}U\omega^* \end{aligned} \tag{9}$$

Then the basic equations are rewritten as

$$-\frac{\partial}{\partial t}(\nabla^2 \boldsymbol{\Psi}) + (\mathbf{v} \cdot \nabla)\boldsymbol{\omega} - (\boldsymbol{\omega} \cdot \nabla)\mathbf{v} - \frac{1}{Re}\nabla^2 \boldsymbol{\omega} + \frac{Gr}{Re^2}\nabla\theta \times \mathbf{g} = 0 \tag{10}$$

$$\boldsymbol{\omega} + \nabla^2 \boldsymbol{\Psi} = 0 \tag{11}$$

$$\frac{\partial \theta}{\partial t} + (\mathbf{v} \cdot \nabla)\theta - \frac{1}{Pe}\nabla^2 \theta = 0 \tag{12}$$

For simplicity the symbol * indicating non-dimensional values will be dropped, hereafter.

2.3. *Two dimensional formulation*

In Cartesian (x, y, z) co-ordinates, equations (10)–(12) are reduced, for two dimensional plane (x, y) equations, as follows. Equations (4) and (7) mean that $\boldsymbol{\Psi}$ and $\boldsymbol{\omega}$ can be represented by their z-components alone as

$$\boldsymbol{\Psi} = (0, 0, \psi(x, y)), \qquad \boldsymbol{\omega} = (0, 0, \omega(x, y)) \tag{13}$$

Then, equations (4) and (11) give

$$v_x = \partial\psi/\partial y, \qquad v_y = -\partial\psi/\partial x \tag{14}$$

$$\frac{\partial^2 \psi}{\partial x^2} + \frac{\partial^2 \psi}{\partial y^2} + \omega = 0 \tag{15}$$

Considering the incompressibility and the following relation

$$\nabla \cdot (\mathbf{v}\omega) = \omega(\nabla \cdot \mathbf{v}) + (\mathbf{v} \cdot \nabla)\omega \tag{16}$$

the z-component of equation (10) gives

$$-\frac{\partial}{\partial t}\left(\frac{\partial^2\psi}{\partial x^2}+\frac{\partial^2\psi}{\partial y^2}\right)+\frac{\partial}{\partial x}(v_x\omega)+\frac{\partial}{\partial y}(v_y\omega)-\frac{1}{Re}\left(\frac{\partial^2\omega}{\partial x^2}+\frac{\partial^2\omega}{\partial y^2}\right)-\frac{Gr}{Re^2}\left(g_x\frac{\partial\theta}{\partial y}-g_y\frac{\partial\theta}{\partial x}\right)=0 \tag{17}$$

Similarly, equation (12) gives

$$\frac{\partial\theta}{\partial t}+\frac{\partial}{\partial x}(v_x\theta)+\frac{\partial}{\partial y}(v_y\theta)-\frac{1}{Pe}\left(\frac{\partial^2\theta}{\partial x^2}+\frac{\partial^2\theta}{\partial y^2}\right)=0 \tag{18}$$

2.4. Boundary conditions

Many studies, based on stream function–vorticity formulation, use the equation of motion of vorticity. Using this formulation, even in FEM studies, not only in FDM ones, some finite difference approximations[3,9,10,11,13] are used for the estimation of the boundary values of vorticity. Hence, the mesh subdivision must be perpendicular to such boundaries. One of the approximations can be written, for example, as follows.[10]

$$\omega_w=-\left\{\frac{3(\psi_w-\psi_i)}{(\Delta n)^2}+\frac{\omega_i}{2}\right\} \tag{19}$$

where subscript i denotes the inner node located on the perpendicular, with the distance of Δn, from the corresponding boundary wall node denoted by the subscript w. It is apparent that the approximation induces numerical errors and reduces the practical convenience.

In order to avoid this difficulty, Ikenouchi and Kimura[14] treated the equation of motion of the stream function instead of the vorticity, in their study of the Navier–Stokes equation without body force. They also used equation (15) only to calculate ω of the convection term of the momentum transport equation. Therefore, they had to solve no differential equation in ω, and needed no boundary condition on ω, on such no-slip boundaries.

We extend this method by coupling equation (17) with the thermal transport equation (18). Four types of boundary conditions for the stream function and two types for the temperature field are used as follows.

Inlet flow boundary	S_1: $\psi=\hat{\psi}$,	$\omega=\hat{\omega}$	(20a)
No-slip boundary	S_2: $\psi=\hat{\psi}$,	$\partial\psi/\partial n=0$	(20b)
Outlet flow boundary	S_3: $\partial\psi/\partial n=0$,	$\partial\omega/\partial n=0$	(20c)
Isolated no-slip boundary	S_4: $\partial\psi/\partial s=0$,	$\partial\psi/\partial n=0$	(20d)
Temperature prescribed boundary	S_5: $\theta=\hat{\theta}$		(21a)
Thermal flux prescribed boundary	S_6: $-\partial\theta/\partial n=\hat{q}_n$		(21b)

The boundaries satisfy the following relations.

$$S=S_1\cup S_2\cup S_3\cup S_4=S_5\cup S_6 \tag{22a}$$

$$S_i\cap S_j=\varnothing \quad (1<i<j<4), \qquad S_5\cap S_6=\varnothing \tag{22b}$$

The right direction of the surface is chosen as that one can see the analysis region on the left hand side. Figure 1 schematically shows the relation between V and $S_1,\ldots,S_4$.

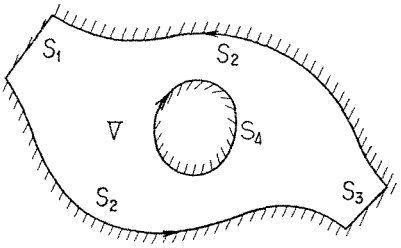

Figure 1. Schematic diagram of analysis region and flow boundaries. V: Analysis region, S_1: Inlet flow boundary, S_2: No-slip boundary, S_3: Outlet flow boundary, S_4: Isolated no-slip boundary. Thermal boundaries S_5 (temperature prescribed boundary) and S_6 (thermal flux prescribed boundary) overlap with boundaries $S_1, \ldots, S_4$

Similar to Ikenouchi and Kimura,[14] boundary values of weighting functions are set as follows.

$$S_1: \ \tilde{\psi} = 0, \qquad \tilde{\omega} = 0 \tag{23a}$$

$$S_2: \ \tilde{\psi} = 0, \qquad \tilde{\omega} = \text{arbitrary} \tag{23b}$$

$$S_3: \ \tilde{\psi} = \text{constant}, \qquad \tilde{\omega} = \text{constant} \tag{23c}$$

$$S_4: \ \tilde{\psi} = \text{constant and arbitrary} \tag{23d}$$

$$S_5: \ \tilde{\theta} = 0, \tag{24a}$$

$$S_6: \ \tilde{\theta} = \text{arbitrary} \tag{24b}$$

2.5. *Discretization with the Galerkin method*

In the FEM formulation of fluid flow, it is common to use weak formulations for the discretizations of the basic equations. Then, equation (17) is multiplied by a weighting function and integrated over the analysis region. Applying Green's theorem and using equation (14) and boundary conditions (20)–(24), we obtain

$$\iint_V \left\{ \frac{\partial \tilde{\psi}}{\partial x}\frac{\partial \dot{\psi}}{\partial x} + \frac{\partial \tilde{\psi}}{\partial y}\frac{\partial \dot{\psi}}{\partial y} + \left(-\frac{\partial \tilde{\psi}}{\partial x}\frac{\partial \psi}{\partial y}\omega + \frac{\partial \tilde{\psi}}{\partial y}\frac{\partial \psi}{\partial x}\omega \right) + \frac{1}{Re}\left(\frac{\partial \tilde{\psi}}{\partial x}\frac{\partial \omega}{\partial x} + \frac{\partial \tilde{\psi}}{\partial y}\frac{\partial \omega}{\partial y} \right) \right.$$

$$\left. - \frac{Gr}{Re^2}\tilde{\psi}\left(g_x\frac{\partial \theta}{\partial y} - g_y\frac{\partial \theta}{\partial x} \right) \right\} dx\, dy = -\int_{S_3} \tilde{\psi} v_n \omega \, ds + \int_{S_4} \frac{1}{Re}\tilde{\psi}\frac{\partial \omega}{\partial n} ds \tag{25}$$

The boundary condition on $\partial\omega/\partial n$ in the second term of the right hand side of equation (25) is eliminated on isolated isothermal boundaries (Appendix I). The first term of the right hand side of equation (25) is evaluated from the value calculated by equation (15), and needs no finite difference approximation.

For the matrix formulation, we expand the weighting functions and variables by interpolation functions N_α and N_β as follows.

$$\begin{aligned} \tilde{\psi} &= \tilde{\psi}_\alpha N_\alpha, \quad & \tilde{\omega} &= \tilde{\omega}_\alpha N_\alpha, \quad & \tilde{\theta} &= \tilde{\theta}_\alpha N_\alpha \\ \psi &= \psi_\beta N_\beta, \quad & \omega &= \omega_\beta N_\beta, \quad & \theta &= \theta_\beta N_\beta \end{aligned} \tag{26}$$

It is mathematically equivalent to use N_α and N_β instead of the original variables and weighting functions.[9] Then we obtain the following matrix equation.

$$A_{\alpha\beta}\dot{\psi}_\beta + B_{\alpha\beta\gamma}\psi_\beta\omega_\gamma + C_{\alpha\beta}\omega_\beta + D_{\alpha\beta}\theta_\beta = E_\alpha \tag{27}$$

In a similar and more straightforward manner, we discretize equations (15) and (18), respectively as

$$F_{\alpha\beta}\psi_\beta + G_{\alpha\beta}\omega_\beta = 0 \tag{28}$$

$$P_{\alpha\beta}\dot{\theta}_\beta + Q_{\alpha\beta\gamma}\psi_\beta\theta_\gamma + R_{\alpha\beta}\theta_\beta = S_\alpha \tag{29}$$

The detailed definitions of the matrices and vectors $A_{\alpha\beta}, \ldots, S_\alpha$ are listed in Appendix II.

3. NUMERICAL TECHNIQUES

We use first order isoparametric interpolation functions. For surface integration, we use Radon type 7-points numerical integration which calculates polynomials below 5th order with no error, and for line integral we use first order error Gauss–Legendre numerical integration.

In order to suppress the instability of computation with high Reynolds and Grashoff numbers, and to make the calculation efficient, we replace the weighting function N_α of convection terms $B_{\alpha\beta\gamma}$ and $Q_{\alpha\beta\gamma}$ by upwind weighting functions[9] considering the element Reynolds and Peclet numbers. For time integration, we use explicit techniques: Euler method and 2-step Lax–Wendroff method. Expressing time dependent matrix equations generally as

$$\mathbf{M}\dot{\mathbf{u}} + \mathbf{K}(\mathbf{u})\mathbf{U} = \mathbf{F} \tag{30}$$

and supposing that the value of $\mathbf{u}$ at the time step n is known, the value of $\mathbf{u}$ at the next step is calculated by the 2-step Lax–Wendroff method as

$$\mathbf{u}^{n+\frac{1}{2}} = \mathbf{u}^n + \frac{\Delta t}{2}\mathbf{M}^{-1}\{\mathbf{F}^n - \mathbf{K}(\mathbf{u}^n)\mathbf{u}^n\} \tag{31a}$$

$$\mathbf{u}^{n+1} = \mathbf{u}^n + \Delta t\mathbf{M}^{-1}\{\mathbf{F}^n - \mathbf{K}(\mathbf{u}^{n+\frac{1}{2}})\mathbf{u}^{n+\frac{1}{2}}\} \tag{31b}$$

where superscripts n, $n+1$, and $n+\frac{1}{2}$ indicate the values at the time step n, $n+1$, and the middle of the time steps n and $n+1$. The computing flow diagram is illustrated by Figure 2.

4. NUMERICAL RESULTS

4.1. Natural convection in a closed cavity

This problem is a recirculatory convection induced by a hot wall with the other wall kept to lower temperature, and with top and bottom walls insulated. Calculation was performed for $Re = 10^5$ with and without upwind weighting functions.

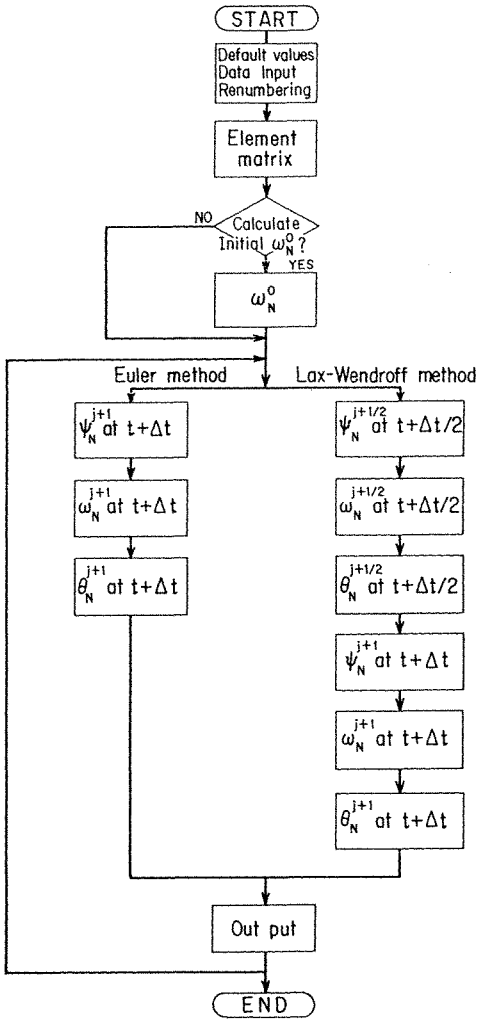

Figure 2. Flow diagram of the computation

Figures 3(a) and (b) show the isotherms and stream function of the almost stationary solution without the use of the upwind weighting function. A similar solution was obtained when we used the upwind treatment.

The two crosses in Figure 3(b) denote the vortex centres of the time independent solutions of Reddy and Satake.[13]

The calculation of the almost stationary solution needed the physical time of 36 s. The CPU time and allowable time intervals were 9 min and 5×10^{-2}–10^{-1} s with the upwind treatment, and 370 min and 10^{-3}–5×10^{-3} s without the treatment. Comparing the two methods of time integration, we found little difference in calculation efficiency.

4.2. Natural convection around a horizontal hot cylinder

As the preparation for the analysis of the convection of air around the JT-60 vacuum vessel, we calculated a problem with some resemblance: the natural convection of air

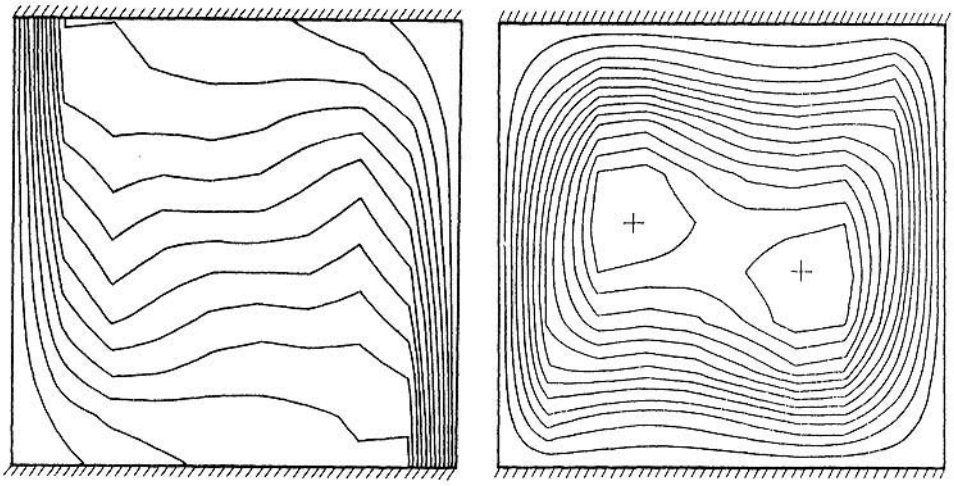

Figure 3. Almost stationary solution of natural convection in a closed cavity. Induced by the right-hand-side hot wall with the other wall kept to be cold ($Re = 10^5$). (a) Isotherms of normalized temperature. (b) Stream function—two crosses denote the vortex centres of the calculation of Reddy and Satake[13]

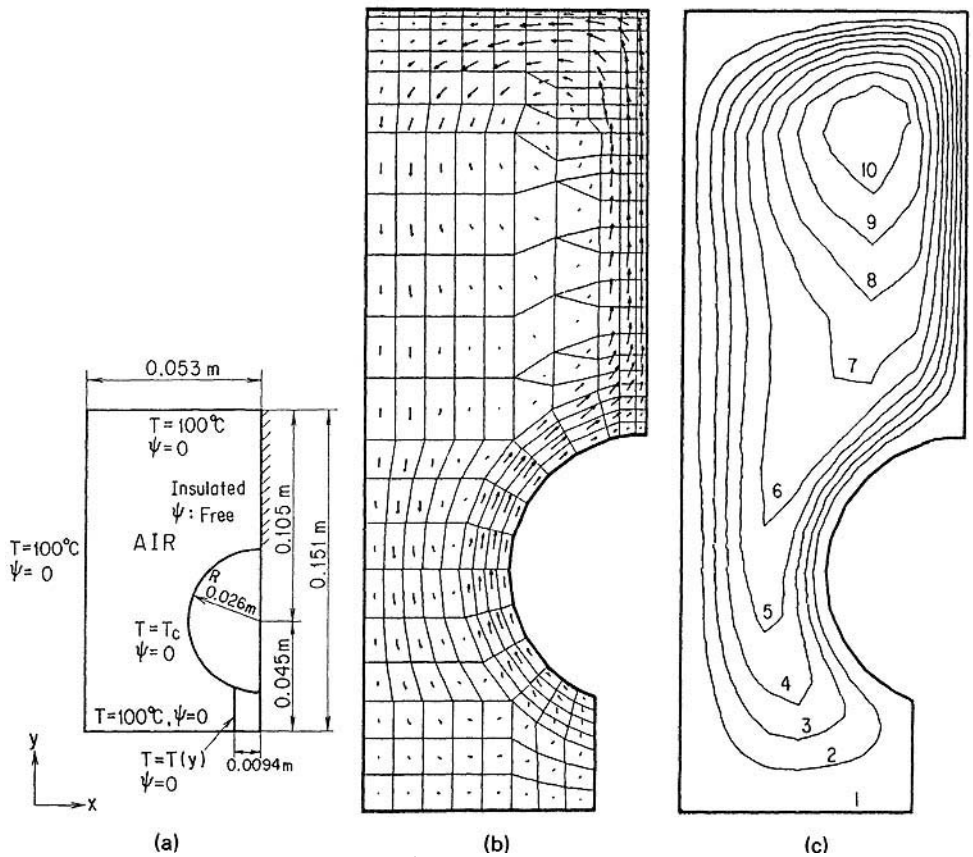

Figure 4. Natural convection around a horizontal hot cylinder placed in a rectangular closed cavity. (a) Geometry of the analysis region. The left half region is analysed because of the symmetry of the problem. The stream function ψ is set to be 0 on the boundary except on the line of symmetry (hatched line) where ψ may vary self-consistently. Convection is induced by the hot cylinder. The temperature on the rectangular cavity is 100°C, and the support temperature spatially change from 100°C to T_c, the temperature of the cylinder surface. The line of symmetry is thermally insulated. (b) Mesh subdivision and flow vectors of the almost stationary solution with $T_c = 110$°C and $Gr = 0{\cdot}8 \times 10^5$. (c) Stream function of the almost stationary solution with $T_c = 110$°C and $Gr = 0{\cdot}8 \times 10^5$

induced by a horizontal hot cylinder placed in a rectangular closed cavity. Because of the symmetry of the geometry, we analysed only the left region illustrated by Figure 4(a). We set the boundary value on ψ as 0 (no-slip boundary) except on the line of symmetry over the cylinder where ψ may change self-consistently. The temperature of the rectangular boundary is 100°C, and the temperature on the boundary of the cylinder support is set to spatially change from 100°C to T_c, the temperature of the cylinder. The line of symmetry of the fluid region is thermally isulated.

Considering the complexity of the problem, we used the upwind treatment. When we set T_c to be 200°C, the computation diverged after the evolution of initial flow. Hence, we divided the temperature difference between the cylinder and the cavity into small increments of 10°C, to obtain a stable computation. The almost stationary solution of the latest incremental step was used as the initial condition of the next incremental step. After the repetition of the incremental steps, we obtained the almost stationary solution of natural convection with $T_c = 140$°C and $Gr = 2 \times 10^5$. Figure 4(b) shows the mesh with flow vectors of the almost stationary solution with $T_c = 110$°C. We used small mesh subdivision near the upper side of the rectangle and the line of symmetry, in order to stabilize the spatial disorder of the temperature field which was inevitable with more coarse mesh subdivision. Figure 4(c) shows the stream function of the same solution.

Figures 5(a)–(g) show the time evolution and convergence process of the natural convection with $T_c = 110$°C and $Gr = 0{\cdot}8 \times 10^5$. We see the initial evolution of temperature field (Figures 5(a), (b)), the formation of a stagnant region of temperature (Figures 5(c)–(e)), and the process of temperature diffusion towards the almost stationary solution (Figures 5(f), (g)). Figures 6–8 are the isotherms of the almost stationary solutions with $T_c = 120$°C, 130°C and 140°C, respectively. The isotherms show a mushroom-like shape which grows according to the increase of Grashoff number and seems to be characteristic of this geometry. Similar geometry was analysed computationally and experimentally by Gartling and Nickell (G&N)[15] with Grashoff number of 4×10^5. Compared with their isotherms, ours are sharper and more complex, partly because our mesh is finer where spatial change of temperature field is large. Considering the ambiguity of the holometric photograph of G&N and the limitation of our plotter program, our results are almost as the same as that of G&N with similar geometry and a little different parameter.

For numerical computation, we used FACOM M200 at JAERI computer centre. The number of iterations and the CPU time, necessary for the almost stationary solution with $T_c = 110$°C, were about 1200 and 15 h, respectively. The time intervals were from 10^{-3} s to 5×10^{-3} s. According as T_c was increased, shorter time intervals were necessary.

5. CONCLUSIONS

This paper has presented an advanced method for the analysis of 2-dimensional transient natural convection, with arbitrary mesh subdivision on no-slip boundaries. It was confirmed that the upwind weighting function suppressed spatial disorder of temperature distribution and accelerated the time integration of such highly non-linear problems as natural convection.

We are intending to apply the present method to the natural convection around the vacuum vessel of JT-60, by extending the method to cylindrical problems and including some additional boundary conditions.

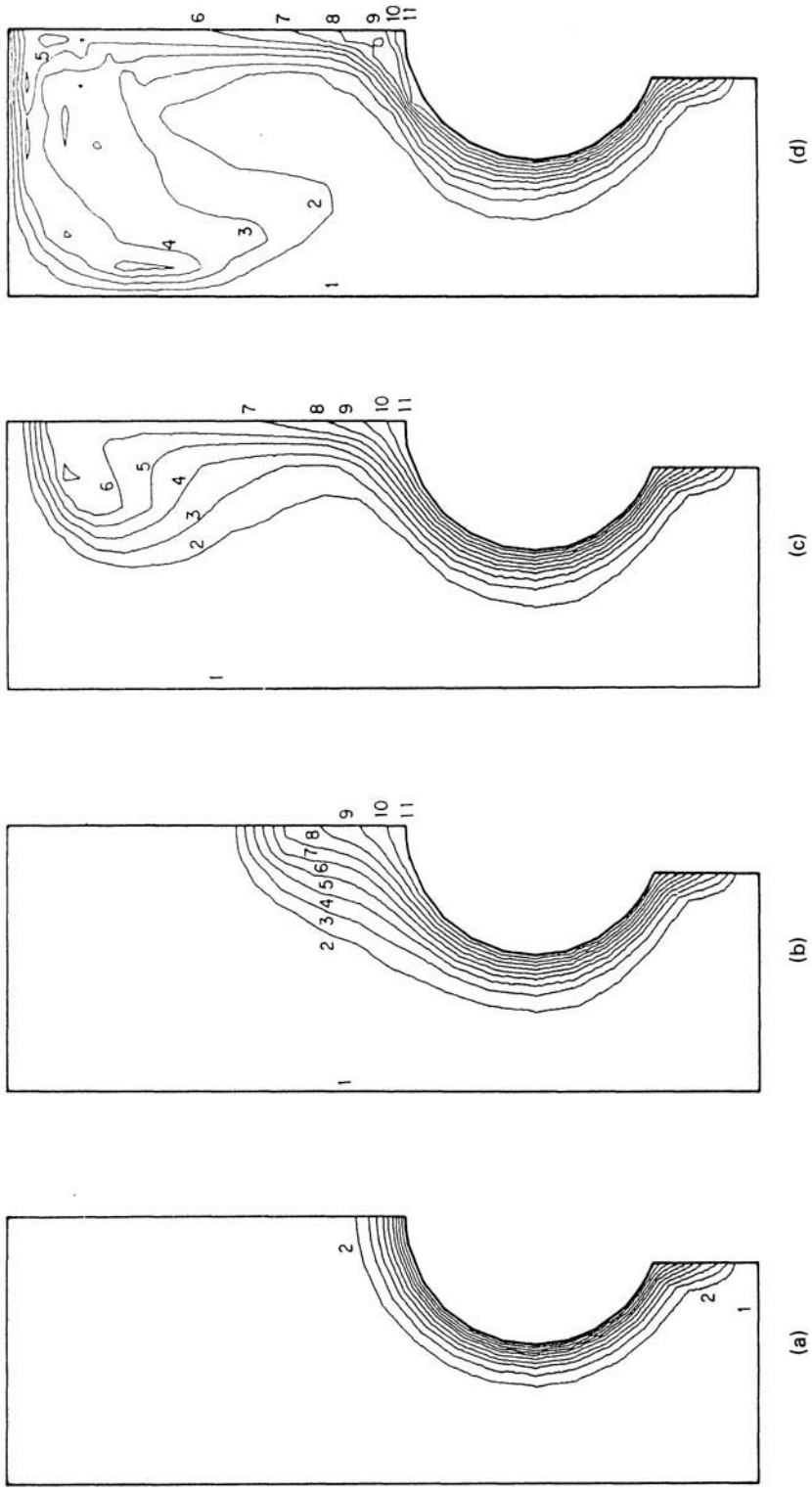
(a)
(b)
(c)
(d)

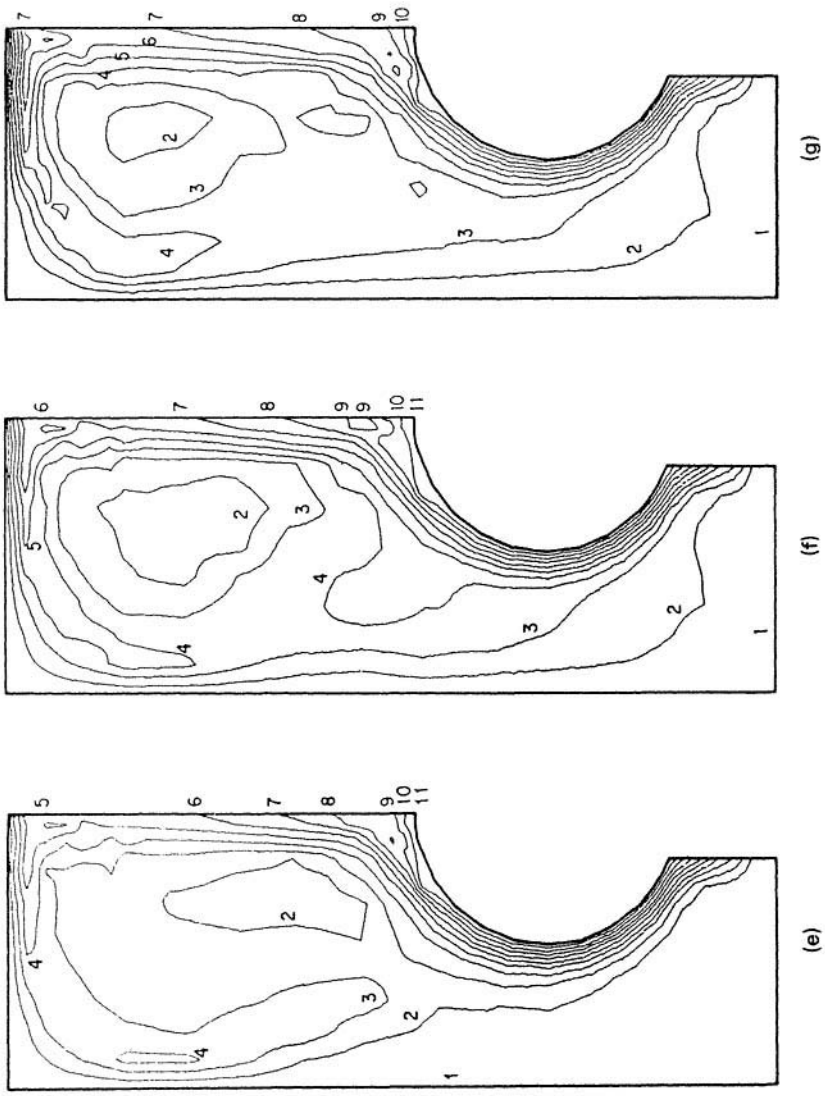

Figure 5. Time dependent evolution of temperature field with $T_c = 110°C$. Isotherms have the values from 100°C (line 1) to 110°C (line 11) with equal intervals. (a) Isotherms with the physical time of 2 s. (b) Isotherms with the physical time of 4 s. (c) Isotherms with the physical time of 6 s. (d) Isotherms with the physical time of 8 s. (e) Isotherms with the physical time of 10 s. (f) Isotherms with the physical time of 20 s. (g) Isotherms of the almost stationary solution

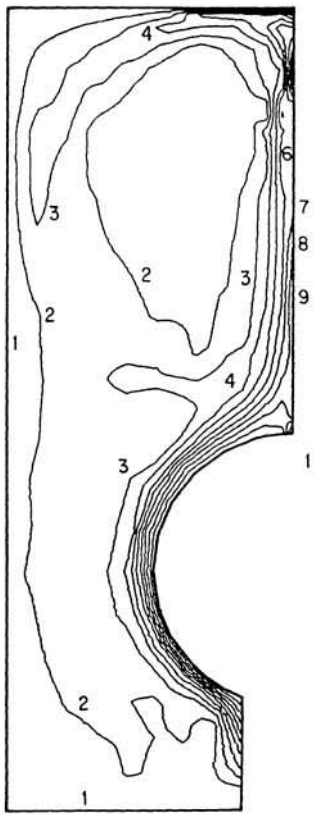

Figure 6. Almost stationary solution with $T_c = 120°C$ and $Gr = 1{\cdot}5 \times 10^5$. Isotherms which have the values from 100°C (line 1) to 120°C (line 11) with equal intervals

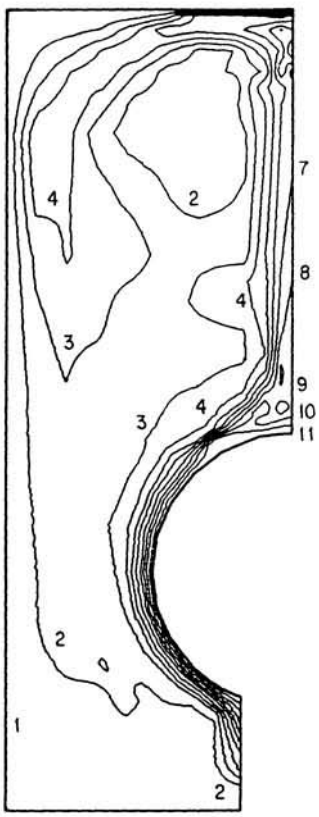

Figure 7. Almost stationary solution with $T_c = 130°C$ and $Gr = 2 \times 10^5$. Isotherms which have the values from 100°C (line 1) to 130°C (line 11) with equal intervals

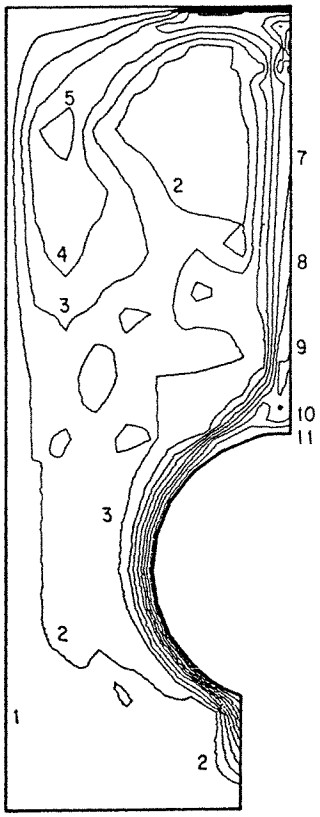

Figure 8. Almost stationary solution with $T_c = 140°C$ and $Gr = 2 \times 10^5$. Isotherms which have the values from 100°C (line 1) to 140°C (line 11) with equal intervals

ACKNOWLEDGEMENT

We would like to acknowledge the kind guidance and encouragement of Dr. G. Yagawa, The University of Tokyo, Drs. M. Yoshikawa, T. Iijima and M. Ohta, Division of Large Tokamak Development, Dr. M. Kuriyama, Division of Fusion Research, and Mr. N. Saito, Computer Center, JAERI. We are also obliged to Mr. T. Shimizu, Ishikawajima-Harima Heavy Industries Co., Ltd., for his computational assistance.

NOMENCLATURE

a	thermal diffusivity	p	pressure deviation
$Gr = g\beta\Delta TL^3/\nu^2$	Grashoff number	q_i	ith component of heat flux
$\mathbf{g}$	gravity acceleration vector		
g	gravity acceleration	$Ra = Gr \cdot Pr$	Rayleigh number
L	reference value of length	$Re = UL/\nu$	Reynolds number
N_α	interpolation function	S, S_1–S_6	boundaries of analysis region
n	time step		
n_i	ith component of unit normal vector	$\mathbf{s}$	unit tangential vector
		s	tangential line element
$Pe = UL/a$	Peclet number	T	temperature deviation
$Pr = \nu/a$	Prandtl number	T_∞	ambient temperature

t time
U reference value of velocity
$\mathbf{u}$ general vector variable
V analysis region
v_i ith component of velocity
$x_i (i = 1, 2)$ ith component of co-ordinates
α, β, γ nodes
β coefficient of volumetric expansion
ΔT reference value of temperature difference
Δt time step
θ non-dimensional temperature deviation
κ thermal conductivity
ν kinematic viscosity
ρ density
$\varnothing$ null set
$\boldsymbol{\Psi}$ vector potential
ψ stream function
$\boldsymbol{\omega}$ vorticity vector
ω vorticity
$(\tilde{\ })$ weighting function
$(\ )_i$ ith component of vector $(\underset{\sim}{\ })$, or value at an inner node
$(\ )_{,i}$ spatial derivative $\partial(\ )/\partial x_i$
$(\ )_w$ value on the wall
$(\ )_{\alpha(\beta,\gamma)}$ value at node $\alpha(\beta, \gamma)$
$(\ )^*$ non-dimensional value
$(\dot{\ })$ time derivative $\partial(\ )/\partial t$

APPENDIX I. ELIMINATION OF THE BOUNDARY CONDITION OF VORTICITY ON NO-SLIP ISOLATED BOUNDARIES

In order to avoid the boundary condition of ω on no-slip isolated boundaries, we use the uniqueness of pressure as follows. On fixed boundaries, $(\partial \mathbf{v}/\partial t) + (\mathbf{v} \cdot \nabla)\mathbf{v}$ vanishes, and the non-dimensional form of equation (1) yields

$$\nabla p = -\frac{1}{Re}\left(\nabla \times \boldsymbol{\omega} + \frac{Gr}{Re}\mathbf{g}\theta\right) \tag{32}$$

Integration of equation (32) on a boundary gives the pressure difference as

$$\delta p = -\int \frac{1}{Re}\left\{\mathbf{s} \cdot (\nabla \times \boldsymbol{\omega}) + \frac{Gr}{Re}(\mathbf{g} \cdot \mathbf{s})\theta\right\} \mathrm{d}s \tag{33}$$

As δp must be zero on a closed boundary (uniqueness of pressure), we obtain

$$\oint \frac{\partial \omega}{\partial n}\,\mathrm{d}s = \oint \frac{Gr}{Re}\,\theta(\mathbf{g} \cdot \mathbf{s})\,\mathrm{d}s \tag{34}$$

where the property $\mathbf{s} \cdot (\nabla \times \boldsymbol{\omega}) = -\partial\omega/\partial n$ (in $x - y$ co-ordinates) was used. Hence, the second term of the right hand side of equation (24) is evaluated on an isolated boundary where the temperature is constant as

$$\frac{1}{Re}\oint_{S_4} \partial\omega/\partial n\,\mathrm{d}s = \frac{Gr}{Re^2}\,\theta \oint_{S_4} (\mathbf{g} \cdot \mathbf{s})\,\mathrm{d}s = 0 \tag{35}$$

APPENDIX II. DETAILED DEFINITION OF MATRICES

The matrices of equations (27), (28) and (29) are defined by the following equations.

$$A_{\alpha\beta} = \iint_V \left(\frac{\partial N_\alpha}{\partial x}\frac{\partial N_\beta}{\partial x} + \frac{\partial N_\alpha}{\partial y}\frac{\partial N_\beta}{\partial y}\right) \mathrm{d}x\,\mathrm{d}y \tag{36}$$

$$B_{\alpha\beta\gamma} = \iint_V \left(-\frac{\partial N_\alpha}{\partial x}\frac{\partial N_\beta}{\partial y} + \frac{\partial N_\alpha}{\partial y}\frac{\partial N_\beta}{\partial x} \right) N_\gamma \, dx \, dy \tag{37}$$

$$C_{\alpha\beta} = \iint_V \frac{1}{Re} \left(\frac{\partial N_\alpha}{\partial x}\frac{\partial N_\beta}{\partial x} + \frac{\partial N_\alpha}{\partial y}\frac{\partial N_\beta}{\partial y} \right) dx \, dy \tag{38}$$

$$D_{\alpha\beta} = -\iint_V \frac{Gr}{Re^2} N_\alpha \left(g_x \frac{\partial N_\beta}{\partial y} - g_y \frac{\partial N_\beta}{\partial x} \right) dx \, dy \tag{39}$$

$$E_\alpha = -\int_{S_3} N_\alpha v_n \omega \, ds$$

$$F_{\alpha\beta} = -A_{\alpha\beta} \tag{40}$$

$$G_{\alpha\beta} = \iint_V N_\alpha N_\beta \, dx \, dy \tag{41}$$

$$P_{\alpha\beta} = G_{\alpha\beta} \tag{42}$$

$$Q_{\alpha\beta\gamma} = B_{\alpha\beta\gamma} \tag{43}$$

$$R_{\alpha\beta} = \iint_V \frac{1}{Pe} \left(\frac{\partial N_\alpha}{\partial x}\frac{\partial N_\beta}{\partial x} + \frac{\partial N_\alpha}{\partial y}\frac{\partial N_\beta}{\partial y} \right) dx \, dy \tag{44}$$

$$S_\alpha = \int_{S_6} N_\alpha \left(\frac{1}{Pe}\frac{\partial \theta}{\partial n} - \theta v_n \right) ds \tag{45}$$

REFERENCES

1. T. D. Richtmyer and K. W. Morton, *Difference Methods for Initial-value Problems*, 2nd edn., Interscience, London, 1973.
2. D. Potter, *Computational Physics*, Wiley, London, 1973.
3. P. J. Roache, *Computational Fluid Dynamics*, Hermosa, Albuquerque, 1976.
4. G. de Vahl Davis and G. D. Mallinson, 'A note on natural convection in a vertical slot', *J. Fluid Mech.*, **72,** (1), 87–93 (1972).
5. J. W. Elder, 'Laminar free convection in a vertical slot', *J. Fluid Mech.*, **23,** (1), 77–98 (1965).
6. G. D. Mallinson and G. de Vahl Davis, 'The method of the false transient for the solution of coupled elliptic equations', *J. Comp. Phys.*, **12,** 435–461 (1973).
7. D. W. Pepper and S. D. Harris, 'Numerical simulation of natural convection in closed containers by a fully implicit method', *Numerical/Laboratory computer method in fluid mechanics (presented at the winter annual meeting of the ASME)*, 181–207, New York (December 1976).
8. K. E. Torrance and J. A. Rockett, 'Numerical study of natural convection in an enclosure with localized heating from below—creeping flow to the onset of laminar instability', *J. Fluid. Mech.*, **36,** (1), 33–54 (1969).
9. O. C. Zienkiewicz, *The Finite Element Method*, McGraw-Hill, London, 1977.
10. J. J. Connor and C. A. Brebbia, *Finite Element Techniques for Fluid Flow*, Butterworth, London, 1976.
11. T. J. Chung, *Finite Element Analysis in Fluid Dynamics*, McGraw-Hill, New York, 1978.
12. R. H. Gallagher, O. C. Zienkiewicz, J. T. Oden, M. M. Cecchi, and C. Taylor (Eds.), *Finite Elements in Fluids—vol. 3*, Wiley, Chichester, 1978.
13. J. N. Reddy and Akio Satake, 'A comparison of a penalty finite element model with the stream function–vorticity model of natural convection in enclosures', *J. Heat Transfer*, **102,** 659–666 (1980).
14. M. Ikenouchi and N. Kimura, 'An approximate numerical solution of the Navier–Stokes equations by Galerkin method', in J. T. Oden, O. C. Zienkiewicz, R. H. Gallagher and C. Taylor (Eds.), *Finite Element Method in Flow Problems*, 99–100, UAH Press, Huntsville, 1974.
15. D. K. Gartling and R. E. Nickell, 'Finite element analysis of free and forced convection', in R. H. Gallagher *et al.* (Eds.), *Finite elements in fluids—vol. 3*, 105–121, Wiley, Chichester, 1978.